



10 World Conference on Neutron Radiography 5-10 October 2014

Neutron Bragg edge tomography for phase mapping

Robin Woracek^{a,*}, Dayakar Penumadu^a, Nikolay Kardjilov^b, Andre Hilger^b, Mirko Boin^b, John Banhart^b, Ingo Manke^b

^aCollege of Engineering, The University of Tennessee, 325 John D Tickle Bldg, Knoxville, TN, 37996, USA

^bInstitute of Applied Materials, Helmholtz-Zentrum Berlin, Hahn-Meitner-Platz 1, 14109 Berlin, Germany

Abstract

This paper describes non-destructive three-dimensional (3D) mapping of crystallographic phase distributions within the bulk (centimeter range) of samples with micrometer-scale resolution. The technique leverages diffraction contrast due to Bragg scattering and the large penetration power of neutrons through high-atomic-number-element-based structural materials. Our tomographic approach overcomes critical limitations of existing techniques by allowing spatially resolved phase mapping in bulk samples and offers a wide range of potential applications. The technique is demonstrated for (metastable 304L stainless) steel samples that exhibit strain-induced martensitic phase transformation after being subjected to tensile and torsional deformation. The distribution of phase fractions within the 3D reconstructed volumes was verified at select locations using neutron diffraction as well as EBSD, and results agree with transformation kinetics theory.

© 2015 The Authors. Published by Elsevier B.V. This is an open access article under the CC BY-NC-ND license (<http://creativecommons.org/licenses/by-nc-nd/4.0/>).

Selection and peer-review under responsibility of Paul Scherrer Institut

Keywords: phase mapping; crystallographic characterization; phase transformation; non-destructive testing; phase tomography; neutron imaging

1. Introduction

1.1. Polycrystalline materials and available characterization techniques

A vast majority of materials which are used for structural support and related engineering applications are polycrystalline metallic alloys. Characterization of polycrystalline materials, in particular their micro-

* Corresponding author, phone: +1-865-974-7708 ; fax: +1-865-974-2669 .
E-mail address: rworacek@utk.edu

structural properties and their state of stress, is of tremendous significance and interest. Established characterization techniques for example include light microscopy (metallography), electron microscopy (transmission electron microscopy and scanning electron microscopy), electron backscatter diffraction (EBSD) and (laboratory) X-ray diffraction. However, all of these techniques are mostly limited to evaluating the surface features and require the sample to be extracted from the bulk requiring destructive specimen preparation approach and only represent small volume observed that is no longer in an undisturbed state. Hard X-rays (for example at a synchrotron source) can penetrate deep into most metals, with certain limitations (Hutchings *et al.*, 2005). While X-rays and electrons interact with the electrons of an atom, neutrons interact with the nucleus and hence neutron radiation provides the ability to penetrate deep into most structural materials. As such, neutron diffraction for instance is considered the only true bulk investigation technique for stress and strain measurements (Allen *et al.*, 1985; Hutchings *et al.*, 2005; Clausen *et al.*, 2003). Electron and X-ray based imaging techniques are very popular amongst scientists and engineers as they provide spatial information, and through a combination with scattering and diffraction modes have evolved to be very powerful and versatile characterization and analysis tools. This makes it possible to perform chemical analysis (Energy-dispersive X-ray spectroscopy, EDS (Goldstein *et al.*, 2003)) and enables crystallographic investigations for grain, strain and phase mapping (EBSD (Goldstein *et al.*, 2003)). It should be noted that especially in the field of diffraction-based imaging using (synchrotron) X-rays, tremendous advances have been made within the last decade for non-destructive three-dimensional (3D) microstructural characterization of crystalline materials, notably differential-aperture X-ray microscopy (DAXM; (Larson *et al.*, 2002)), 3D-X-ray diffraction (3D-XRD; (Poulsen, 2004)) and Diffraction Contrast Tomography (DCT; (Ludwig *et al.*, 2009)). However, even these techniques are still limited to relatively small size sample while neutrons are optimal for bulk investigations (Banhart, 2008). Characterizing the bulk properties is crucial to understanding the meso-scale effects for polycrystalline materials (Doherty *et al.*, 1997).

1.2. Neutron Bragg edge spectroscopy (1D) and imaging (2D)

Information related to the crystal structure of crystalline materials (strain, phase, texture) is traditionally obtained using (X-ray or neutron) diffractometers. In a diffractometer where a fixed wavelength is used, the diffraction angle is determined. If a wavelength spectrum is available (typically at neutron spallation sources), a wavelength-dependent intensity spectrum is recorded under some fixed angle to the direction of the incident neutron beam. The detected intensity maxima (so-called Bragg peaks) are accordingly plotted as a function of diffraction angle or wavelength.

In transmission based Bragg edge imaging, scattering information is contained in the recording of the transmitted neutron beam through the sample: Some neutrons travel without interaction through the sample, some are absorbed, while those that are scattered out of the direction of the incident beam (which are usually detected in a diffractometer configuration), leave a characteristic pattern in the incident intensity spectrum, so-called Bragg edges. Hence, spatial information in two dimensions can be obtained if an imaging detector is used.

Performing Bragg edge transmission imaging with a detector positioned behind the sample, requires the possibility to record the transmitted neutron intensity as a function of wavelength. For a particular hkl family, the scattering angle increases as the wavelength is increased until the Bragg scattering condition cannot be fulfilled any longer, which occurs for wavelengths larger than $\lambda = 2d_{hkl}\sin 90^\circ = 2d_{hkl}$. At this particular wavelength, the transmitted intensity increases drastically (the so called Bragg edge: see Fig. 1). Changes in d_{hkl} would shift the Bragg edge correspondingly, and consequently, strains along the beam direction ($\theta_{hk}^B = 90^\circ$) can be resolved, for “strain radiography” applications. Analogous to a diffraction pattern, phase and texture differences will also lead to differences in the Bragg edge spectrum. Two different phases of iron are shown in Fig. 2a.

Early experiments to study the nuclear cross-sections of elements, using transmission measurements, have been reported by Fermi (Fermi *et al.*, 1947) and Winsberg (Winsberg *et al.*, 1949). The development of the Bragg edge transmission technique continued at reactor sources (Weiss *et al.*, 1952; Cassels, 1950; Mikula *et al.*, 1995; Wagner *et al.*, 1997; Strunz *et al.*, 1997) and spallation sources (Johnson *et al.*, 1982). The next generation of spallation sources installed at Los Alamos National Laboratory (USA; LANSCE) and Rutherford Appleton Laboratory (UK; ISIS), provided unprecedented opportunities. At LANSCE, Meggers, Priesmeyer et al. studied the phase transformation of austenite to bainite in gray iron in real time. (Meggers *et al.*, 1994a; Meggers *et al.*,

1994b) At ISIS, Wang studied in-situ (tensile and compressive) loading of steel samples measured by neutron transmission and compared results with surface strain gauges (Wang, 1996). The Bragg edge transmission technique was further developed at LANSCE, with a focus to investigate kinetics of structural phase transitions, and at ISIS, with a focus on the measurement of d-spacings and strain. Some notable publications as a part of these developments at LANSCE and ISIS include the work by Priesmeyer (Priesmeyer *et al.*, 1999) and Santisteban (Santisteban *et al.*, 2002b), as well as publications from the dissertation research of Vogel at LANSCE (Vogel, 2000) and Steuwer at ISIS (Steuwer *et al.*, 2001; Steuwer *et al.*, 2003). A comparison of Bragg-Edge neutron-transmission spectroscopy at both facilities is reported by both groups (Santisteban *et al.*, 2002c).

Despite these major advancements at spallation sources, a major limitation in transmission imaging resulted from a lack of suitable detector technology, which can provide superior spatial and time resolution. Nonetheless, the term “imaging” was sometimes used in foresight of the developments that should follow. The fundamentals and potentials of crystallographic characterization were demonstrated at the spallation sources LANSCE, ISIS and J-PARC, for the determination of:

- Phases (Vogel, 2000; Steuwer *et al.*, 2005; Santisteban *et al.*, 2002b; Steuwer *et al.*, 2004; Bourke *et al.*, 1996; Huang *et al.*, 2007)
- Texture corresponding to preferential orientation (Santisteban *et al.*, 2006; Iwase *et al.*, 2007; Sato *et al.*, 2010)
- Strain and stress (Steuwer *et al.*, 2003; Santisteban *et al.*, 2001; Steuwer *et al.*, 2001; Santisteban *et al.*, 2002a; Iwase *et al.*, 2012) .

The cited research above either used a single detecting element (no spatial resolution) or relatively coarse pixelated (mm scale) transmission detectors. New detectors are currently being developed for time of flight imaging applications (Kiyonagi *et al.*, 2014; Tremsin *et al.*, 2005; Siegmund *et al.*, 2007; Tremsin *et al.*, 2008).

Several dedicated neutron radiography/tomography instruments at steady state sources can readily provide spatial resolutions on the order of or smaller than 50 μm (Kardjilov *et al.*, 2009) and therefore implementation of energy selective Bragg edge imaging techniques could probe new applications. In principle there are two possibilities to do such energy-dependent measurements at a reactor source (Lehmann *et al.*, 2009): (a) using the time-of-flight information in distance from the source using a specifically designed chopper system or (b) selection (or suppression) of neutrons from specific spectral parts. In the latter case the wavelengths can be selected by a velocity selector, the “slit method” or a wavelength-tunable device, e.g. a double crystal monochromator. Using different settings or crystals allow for a selection of a narrow wavelength regime, but comes with a severe loss of total flux available for imaging.

Proof of principle measurements have been reported at these neutron imaging facilities, for the case of microstructural differences in welds (Kardjilov *et al.*, 2012; Schulz *et al.*, 2009; Lehmann *et al.*, 2009; Josic *et al.*, 2010; Josic *et al.*, 2011), for differentiating materials and strain variations in a bend steel plate (Treimer *et al.*, 2006), for texture effects in a processed aluminium foam sandwich (Kardjilov *et al.*, 2009), for microstructural differences in ancient swords (Salvemini *et al.*, 2012) and historical copper (Peetermans *et al.*, 2012). The majority of the published results, which have been obtained at existing neutron imaging facilities using the Bragg edge method, were largely of qualitative – rather than quantitative – nature. Nonetheless, images recorded in this mode can reveal inhomogeneities and features that would remain undetected otherwise. A comparison of transmission measurements of different welds with electron backscatter diffraction (EBSD) have been performed by the group at PSI (Lehmann *et al.*, 2014).

In 1996, Bourke *et al.* have demonstrated results in bulk changes in transmission Bragg edge spectrum while reversing the phase transformation in austenitic stainless steel, but without an important requirement for having spatial resolution (Bourke *et al.*, 1996). In 2008, the group at HZB (N. Kardjilov, I. Manke, T. Kandemir) demonstrated tomographic reconstructions of metallic samples, which consisted of varying amount of martensite and bainite, but the work has not been published to date. Motivated by these earlier results, the further development of the Bragg edge method was undertaken in joint collaboration between HZB and UTK by the primary authors (Woracek and Penumadu) in this study, with a goal to demonstrate the highly desirable ability to provide quantitative phase mapping in two (radiography) and three dimensions (tomography) of materials.

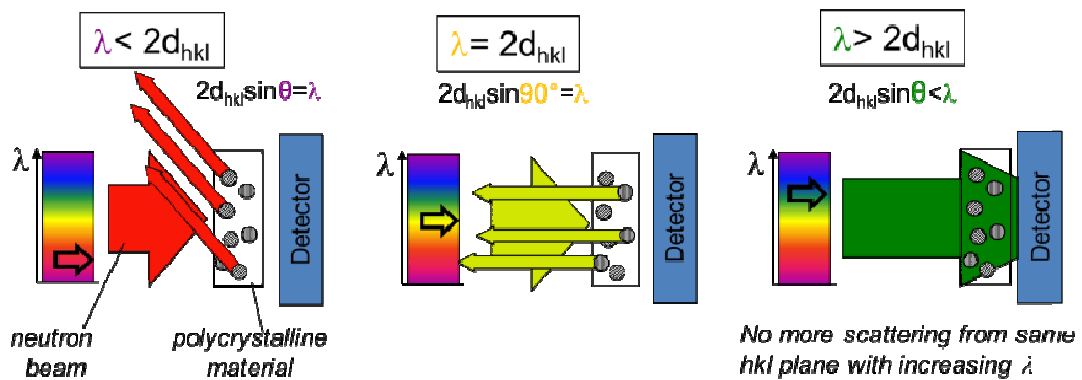


Fig. 1. Principle of Bragg edge radiography: Neutrons of different wavelengths vary in transmitted intensity through polycrystalline samples due to diffraction. This leads to characteristic transmission Bragg edge spectra for crystalline samples. The position of the Bragg edges is directly related to the d-spacing of the lattice planes.

1.3. TRIP effect

The neutron Bragg edge tomography method is demonstrated in this paper using steel samples that exhibit the Transformation induced plasticity (TRIP) effect, which is shortly summarized here. TRIP refers to the transformation of retained face-centered cubic (fcc) austenite (γ) to body-centered cubic bcc (α') and hcp (ϵ) martensite during plastic deformation. Steels that exhibit the TRIP effect have a high ductility, while retaining excellent strength and are hence used in many applications. Due to the excellent formability (through rolling, stamping, drawing etc.), structural components made from TRIP steel can be made thinner while their large amount of work hardening provides high strength (Angel, 1954). Patel & Cohen provide an early overview of the martensitic phase transformation due to applied stress (Patel *et al.*, 1953), while Lo *et al.* give a comprehensive review of recent developments in stainless steel, including the TRIP effect (Lo *et al.*, 2009).

Cakmak reports on “Phase Transformation Kinetics and Texture Evolution in a TRIP Steel under Complex Loads” in his dissertation (Cakmak, 2014), and also provides an excellent review on details about the martensitic phase transformation in general and transformation mechanisms in detail. He summarizes: “In particular, the effective increase in the strain hardening rate due to the in-situ formation of the bcc martensite phase during the deformation helps to prevent premature failure and increase the ductility while maintaining the high strength of the material. In general, the harder bcc martensite phases act as barriers to dislocation motion during straining and enhance the strain hardening rate in this type of alloys (Zackay *et al.*, 1967). The TRIP effect, therefore, helps increase the formability of these alloys, e.g., achieving higher rolling reductions without premature failure since the transformation occurs more readily at locations with the highest strain concentration, and allowing the manufacturing of more complex shapes. However, for enhanced ductility, gradual introduction of the martensite phase is essential because otherwise only the yield strength will increase if the transformation is rapid (Zackay *et al.*, 1967; Jacques *et al.*, 2001). Therefore, the strain-induced martensitic transformation kinetics is an important fundamental and practical issue.”

2. Experimental

2.1. Deformation mode

Tensile testing is ideal to apply a well-known amount of deformation. However for ductile materials (such as TRIP steel), necking often occurs in the center of the gauge area in tensile samples during increased plastic deformation and causes the stress to further concentrate in this region. The torsion test on the other hand allows applying large amounts of deformation without necking. In a cylindrical torsion sample, the maximum shear stress and strain occur towards the outer radius of the cylinder and are zero at its center. The regions of highest strains are

expected to exhibit the largest martensitic phase transformation, and torsional loading thus provides an elegant way of controlling the amount of phase transformation in the radial direction.

Cakmak, Choo et al, have recently published results from a synchrotron diffraction study, and related results are ideally suited to be used as a reference for Bragg edge based measurements. They studied the phase changes from FCC to BCC under torsional loading in 304L stainless steel.(Cakmak *et al.*, 2011) In their study, they used nine separate samples which were plastically deformed to different strain levels and subsequently extracted small portions of the sample for synchrotron diffraction measurements. The phase fractions were then mapped as a function of radial distance from the sample center. This study hence provides an excellent reference for the neutron transmission study presented herein, which is expected to provide phase fraction determination at a lower spatial resolution, but has the advantage of being non-destructive and also cover large sample volumes without sample extraction. For our study, several samples were machined from metastable a stainless steel (ASTM standard 304L) stock of material. Results will be presented in this paper for a non-deformed (VIRGIN) sample, a sample that was plastically deformed under tension (overall engineering strain of 144%) and a samples that was plastically deformed under torsion (maximum shear strain of 250 %). The surface strains were monitored during the deformation by using resistance based rosette strain gauges and by Digital Image Correlation (VIC-3D).

2.2. Neutron transmission experiment

For the results presented here, neutron-imaging beamline CONRAD at the reactor source at Helmholtz-Zentrum Berlin (HZB) was used. The energy selectivity was achieved by employing a tunable double-crystal monochromator consisting of one pyrolytic graphite crystal (PCG) monochromator in the upper and lower position, each with a mosaic spread of 0.8° . The wavelength band has an approximate resolution of $\Delta\lambda/\lambda=3\%$ and can be tuned freely between 2.0 and 6.5 Å while the beam position remains unchanged (Treimer *et al.*, 2006). A neutron detector, based on a ^6LiF scintillator screen of 200 μm thicknesses and an optical CCD camera (2048×2048 pixels) with an objective lens was utilized. The effective pixel size was 53.6 μm , resulting in a $11\times 11\text{ cm}^2$ Field of View (FOV).

The samples were positioned in front of the detector and Bragg edge spectra were obtained for all samples simultaneously in one orientation. The Bragg edge spectra were normalized by the open beam (no sample) image, and the resulting spectra for a region in the sample center is shown in Fig 2b. It can be seen that the middle of the tensile sample is fully transformed to martensite. The average transmission through the middle of the torsion sample shows Bragg edges of both phases. This is expected as the center of the torsion sample does not experience high strain and hence will not transform. Until now, for quantitative evaluation of the phase fractions within this sample, it would need to be destructed. As the next step, tomographic scans were performed by recording 180 projections over a 360° range before (4.1 Å) and after (4.3 Å) the ‘Bragg cut-off’ corresponding to the austenitic phase (more projections would yield even better results, but were not possible in the given time frame). The ‘Bragg cut-off’ for the martensitic phase is slightly shifted towards smaller wavelengths compared to the austenitic phase, resulting in attenuation differences between the two phases in the data taken near 4.1 Å.

The tomographic data was individually reconstructed using filtered back-projection algorithm for parallel beam reconstruction case. The transmitted intensity is higher for regions with larger martensitic phase content due to the different Bragg edge position. The reconstructed data taken at 4.1 Å already provides the 3D crystallographic phase distribution. However, for optimal quantification and to exclude any possible influence of slight material or signal inhomogeneities, the reconstructed slices belonging to 4.1 Å were individually normalized by the reconstructed slices belonging to 4.3 Å. Subsequently, by using a calibration factor corresponding to known weight fractions, phase fraction values are assigned to each voxel and results are shown in Fig 3.

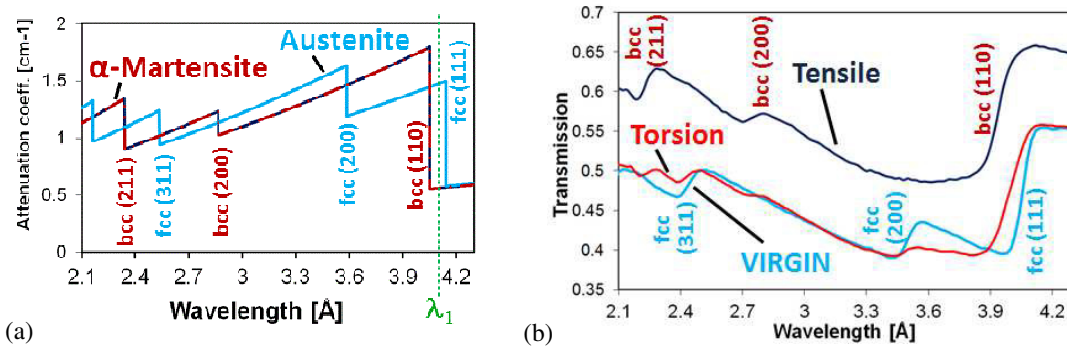


Fig. 2. (a) Theoretical Bragg edge spectra for the Austenite and α -Martensite phases of iron. The depicted wavelength λ_1 will yield a distinct contrast between the two phases. (b) Bragg edge transmission spectra for three different samples: The undeformed sample (VIRGIN) shows only Bragg edges corresponding to the Austenitic phase, while the middle of the tensile sample shows only Bragg edges corresponding to the Martensitic phase. The middle of torsion sample shows Bragg edges corresponding to both phases due to the nature of the strain distribution.

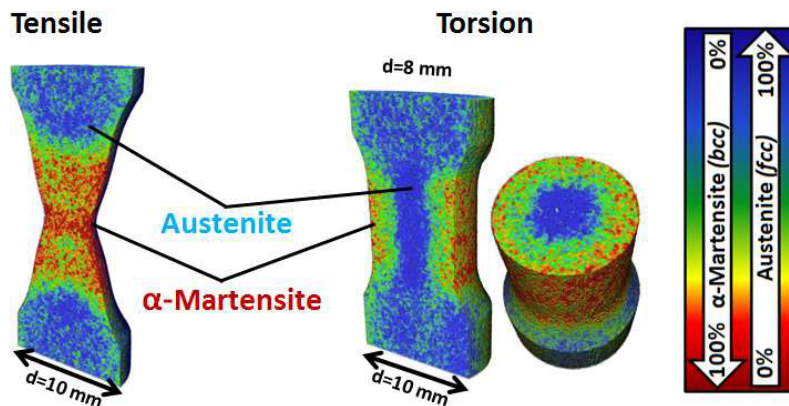


Fig. 3. Tomographic reconstruction of the phase fractions for the tensile and torsion sample. The necking region of the tensile sample is fully transformed to Martensite. The radial dependence of the phase transformation in the torsion sample is revealed and quantified.

2.3. Validation using neutron diffraction and EBSD

With the aim to verify the phase transformation using alternative methods, neutron diffraction and Electron Backscatter Diffraction (EBSD) was performed on these samples. Neutron diffraction was carried out non-destructively at the E3 strain scanner at HZB with the same samples at a few selected locations and results are shown in Fig. 4. EBSD maps were obtained for the various samples, where the un-deformed specimen sections yielded Kikuchi patterns of good quality consistently (>90% indexing success). The scan time to produce an EBSD maps as presented in Fig 5a-b was approximately 45 minutes. The un-deformed samples were mostly austenitic, but some martensite was shown to be present as well, which is expected in such a material. The volume fractions however may not have been enough to be identified by bulk neutron diffraction. Besides the phase determination, the grain size can be seen nicely as well as the grain orientation, also indicating only a low degree of preferred orientation. When investigating areas that are slightly away from the center line of the deformed samples, patches of martensite become apparent. The Kikuchi patterns obtained in regions of the sample that had experienced more strain were of less quality and could often not be indexed. For one region, presented in Fig 5c-d, a scan was performed at a radial distance of 2 mm from the center. In order to obtain data that could be indexed, the electron voltage was reduced, increasing the scan time to over 9 hours. The determined phase fractions at 2 mm (45%

Austenite) agree reasonably well with the ones shown in Fig 4, determined by Bragg edge tomography (one side $\approx 55\%$, the other $\approx 45\%$) and diffraction (one side $\approx 79\%$, the other $\approx 47\%$). One needs to keep in mind that the phase transformation may not happen uniformly throughout and different locations/samples which were probed.

It should be noted that eventually, with more careful preparation and more time consuming scanning procedures (for example further reducing the electron voltage), better EBSD patterns could maybe be obtained in even higher strained regions. Papers addressing deformation of 304 grade stainless steel using EBSD are for example (Shen *et al.*, 2012; Rodríguez-Martínez *et al.*, 2011; Gey *et al.*, 2005; Petit *et al.*, 2007). However, this needs to be considered beyond standard EBSD operation and as such would be methodological development itself. Hence, the neutron imaging approach has a significant advantage of resolving phase fractions in highly strained regions compared to electron backscattered diffraction based approach.

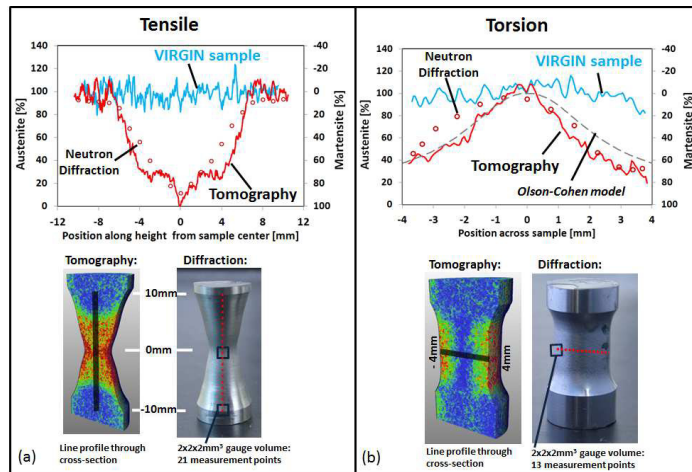


Fig. 4. Quantification of phase fractions depicted using line profiles along and across the reconstructed tomographic data. Neutron diffraction results for a few locations, obtained using a $2 \times 2 \times 2$ mm³ gauge volume and by scanning along/across the samples, are included for a comparison. The diffraction results agree well, but fail to capture sharp gradients due to the relatively large gauge volume. Additionally, the theoretical α -martensite phase evolution is shown using the Olson–Cohen model.

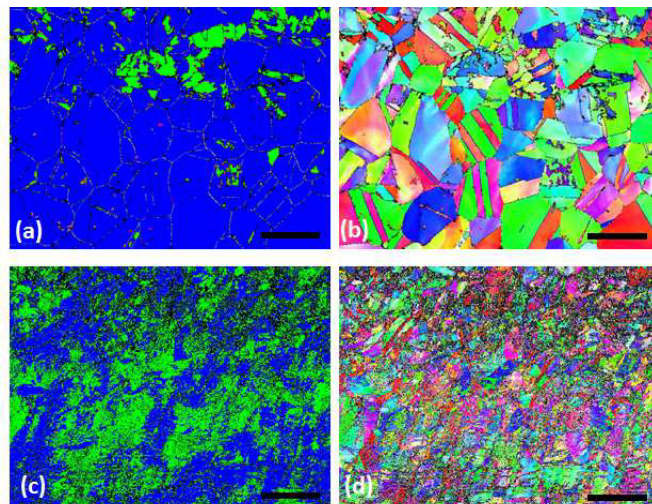


Fig. 5. EBSD phase map (a) and grain orientation map (b) for a un-deformed sample, depicting the sample being mostly austenitic. For the torsion sample at 2mm away from the center, the EBSD phase map (c and d) depicts 45% Austenite. Magnification bar = 30 μ m in all images.

3. Conclusion

Neutron Bragg edge transmission method has been extended for spatially resolved quantitative phase mapping, for characterizing materials noninvasively in three dimensions. This method has the advantage over other established methods, as it is non-destructive, inhomogeneities within large volumes can be detected, and geometric differences such as cracks and holes can be visualized simultaneously with the crystallographic phase identification. Moreover, the method has been proven to be robust and yield data even for highly deformed volumes, where surface methods such as EBSD are problematic. It is anticipated that the Bragg edge tomography technique will find many applications in various fields of science, e.g. physical sciences, materials research, geosciences, biology, and medical sciences. By investigating several Bragg edges simultaneously (either using the time-of-flight or monochromator approach), the accuracy of such measurements can be further improved, while allowing for mapping multiple phases. As an analogy to 3D-XRD and DCT, further developments of this method for the characterization of even highly textured samples are expected using 2 or more detectors in diffraction geometry.

References

- Allen, A. J., Hutchings, M. T., Windsor, C. G. & Andreani, C., 1985. NEUTRON-DIFFRACTION METHODS FOR THE STUDY OF RESIDUAL-STRESS FIELDS. *Advances in Physics* 34, 445-473.
- Angel, T., 1954. Formation of martensite in austenitic stainless steels-effects of deformation, temperature, and composition. *Journal of the iron and steel institute* 177, 165-&.
- Banhart, J. (2008). *Advanced tomographic methods in materials research and engineering*. Oxford University Press New York.
- Bourke, M. A. M., Maldonado, J. G., Masters, D., Meggers, K. & Priesmeyer, H. G., 1996. Real time measurement by Bragg edge diffraction of the reverse ($\alpha' \rightarrow \gamma$) transformation in a deformed 304 stainless steel. *Materials Science and Engineering: A* 221, 1-10.
- Cakmak, E., 2014. Investigation of the Phase Transformation Kinetics and Texture Evolution in a TRIP Steel under Complex Loads.
- Cakmak, E., Choo, H., An, K. & Ren, Y., 2011. Radial distribution of martensitic phase transformation in a metastable stainless steel under torsional deformation: A synchrotron X-ray diffraction study. *Materials Letters* 65, 3013-3015.
- Cassels, J., 1950. The scattering of neutrons by crystals. *Prog. Nucl. Phys.*, editor OR.
- Clausen, B., Leffers, T. & Lorentzen, T., 2003. On the proper selection of reflections for the measurement of bulk residual stresses by diffraction methods. *Acta Materialia* 51, 6181-6188.
- Doherty, R. D., Hughes, D. A., Humphreys, F. J., Jonas, J. J., Jensen, D. J., Kassner, M. E., King, W. E., McNelley, T. R., McQueen, H. J. & Rollett, A. D., 1997. Current issues in recrystallization: a review. *Materials Science and Engineering: A* 238, 219-274.
- Fermi, E., Sturm, W. J. & Sachs, R. G., 1947. The Transmission of Slow Neutrons through Microcrystalline Materials. *Physical Review* 71, 589-594.
- Gey, N., Petit, B. & Humbert, M., 2005. Electron backscattered diffraction study of ϵ/α' martensitic variants induced by plastic deformation in 304 stainless steel. *Metallurgical and Materials Transactions A* 36, 3291-3299.
- Goldstein, J., Newbury, D. E., Joy, D. C., Lyman, C. E., Echlin, P., Lifshin, E., Sawyer, L. & Michael, J. R. (2003). *Scanning electron microscopy and X-ray microanalysis*. Springer.
- Huang, J., Vogel, S. C., Poole, W. J., Militzer, M. & Jacques, P., 2007. The study of low-temperature austenite decomposition in a Fe-C-Mn-Si steel using the neutron Bragg edge transmission technique. *Acta Materialia* 55, 2683-2693.
- Hutchings, M. T., Withers, P. J., T.M.Holden & Lorentzen, T. (2005). *Introduction to the Characterization of Residual Stress by Neutron Diffraction*. CRC Press.
- Iwase, K., Nagata, T., Sakuma, K., Takada, O., Kamiyama, T. & Kiyonagi, Y. (2007). *Nuclear Science Symposium Conference Record, 2007. NSS '07. IEEE*, pp. 1716-1719.
- Iwase, K., Sato, H., Harjo, S., Kamiyama, T., Ito, T., Takata, S., Aizawa, K. & Kiyonagi, Y., 2012. In situ lattice strain mapping during tensile loading using the neutron transmission and diffraction methods. *Journal of Applied Crystallography* 45, 113-118.
- Jacques, P., Furnémont, Q., Mertens, A. & Delannay, F., 2001. On the sources of work hardening in multiphase steels assisted by transformation-induced plasticity. *Philosophical Magazine A* 81, 1789-1812.
- Johnson, R. & Bowman, C., 1982. High resolution powder diffraction by white source transmission measurements. *AIP Conf. Proc.* 89 89, 53-56.
- Josic, L., Lehmann, E. & Kaestner, A., 2011. Energy selective neutron imaging in solid state materials science. *Nuclear Instruments and Methods in Physics Research Section A: Accelerators, Spectrometers, Detectors and Associated Equipment* 651, 166-170.
- Josic, L., Steuwer, A. & Lehmann, E., 2010. Energy selective neutron radiography in material research. *Applied Physics A* 99, 515-522.
- Kardjilov, N., Hilger, A., Manke, I., Strobl, M., Dawson, M. & Banhart, J., 2009. New trends in neutron imaging. *Nuclear Instruments and Methods in Physics Research Section A: Accelerators, Spectrometers, Detectors and Associated Equipment* 605, 13-15.
- Kardjilov, N., Manke, I., Hilger, A., Williams, S., Strobl, M., Woracek, R., Boin, M., Lehmann, E., Penumadu, D. & Banhart, J., 2012. Neutron Bragg-edge mapping of weld seams. *International Journal of Materials Research*, p. 151-154
- Kiyonagi, Y., Kamiyama, T., Kino, K., Sato, H., Sato, S. & Uno, S., 2014. Pulsed neutron imaging using 2-dimensional position sensitive detectors. *Journal of Instrumentation* 9, C07012.
- Larson, B. C., Yang, W., Ice, G. E., Budai, J. D. & Tischler, J. Z., 2002. Three-dimensional X-ray structural microscopy with submicrometre

- resolution. *Nature* 415, 887-890.
- Lehmann, E., Peetermans, S., Josic, L., Leber, H. & van Swygenhoven, H., 2014. Energy-selective neutron imaging with high spatial resolution and its impact on the study of crystalline-structured materials. *Nuclear Instruments and Methods in Physics Research Section A: Accelerators, Spectrometers, Detectors and Associated Equipment* 735, 102-109.
- Lehmann, E. H., Frei, G., Vontobel, P., Josic, L., Kardjilov, N., Hilger, A., Kockelmann, W. & Steuwer, A., 2009. The energy-selective option in neutron imaging. *Nuclear Instruments and Methods in Physics Research Section A: Accelerators, Spectrometers, Detectors and Associated Equipment* 603, 429-438.
- Lo, K. H., Shek, C. H. & Lai, J. K. L., 2009. Recent developments in stainless steels. *Materials Science and Engineering: R: Reports* 65, 39-104.
- Ludwig, W., Reischig, P., King, A., Herbig, M., Lauridsen, E. M., Johnson, G., Marrow, T. J. & Buffière, J. Y. (2009). *Three-dimensional grain mapping by x-ray diffraction contrast tomography and the use of Friedel pairs in diffraction data analysis*. AIP.
- Meggers, K., Priesmeyer, H. G., Trela, W. J., Bowman, C. D. & Dahms, M., 1994a. Real time neutron transmission investigation of the austenite-bainite transformation in grey iron. *Nuclear Instruments and Methods in Physics Research Section B: Beam Interactions with Materials and Atoms* 88, 423-429.
- Meggers, K., Priesmeyer, H. G., Trela, W. J. & Dahms, M., 1994b. Investigation of the austenite-bainite transformation in gray iron using real time neutron transmission. *Materials Science and Engineering: A* 188, 301-304.
- Mikula, P., Vrána, M., Lukáš, P., Šaroun, J., Strunz, P., Wagner, V. & Alefeld, B., 1995. Bragg optics for strain/stress measurement techniques. *Physica B: Condensed Matter* 213–214, 845-847.
- Patel, J. R. & Cohen, M., 1953. Criterion for the action of applied stress in the martensitic transformation. *Acta Metallurgica* 1, 531-538.
- Peetermans, S., van Langh, R., Lehmann, E. & Pappot, A., 2012. Quantification of the material composition of historical copper alloys by means of neutron transmission measurements. *Journal of Analytical Atomic Spectrometry* 27, 1674-1679.
- Petit, B., Gey, N., Cherkaoui, M., Bolle, B. & Humbert, M., 2007. Deformation behavior and microstructure/texture evolution of an annealed 304 AISI stainless steel sheet. *Experimental and micromechanical modeling. International journal of plasticity* 23, 323-341.
- Poulsen, H. F. (2004). *Three-Dimensional X-Ray Diffraction Microscopy: Mapping Polycrystals and their Dynamics*. Heidelberg: Springer.
- Priesmeyer, H. G., Stalder, M., Vogel, S., Meggers, K., Bless, R. & Trela, W., 1999. Bragg-Edge Transmission as an Additional Tool for Strain Measurements. *Textures and Microstructures* 33, 173-185.
- Rodríguez-Martínez, J. A., Pesci, R. & Rusinek, A., 2011. Experimental study on the martensitic transformation in AISI 304 steel sheets subjected to tension under wide ranges of strain rate at room temperature. *Materials Science and Engineering: A* 528, 5974-5982.
- Salvemini, F., Grazzi, F., Peetermans, S., Civita, F., Franci, R., Hartmann, S., Lehmann, E. & Zoppi, M., 2012. Quantitative characterization of Japanese ancient swords through energy-resolved neutron imaging. *Journal of Analytical Atomic Spectrometry* 27, 1494-1501.
- Santisteban, J. R., Edwards, L., Fitzpatrick, M. E., Steuwer, A., Withers, P. J., Daymond, M. R., Johnson, M. W., Rhodes, N. & Schooneveld, E. M., 2002a. Strain imaging by Bragg edge neutron transmission. *Nuclear Instruments and Methods in Physics Research Section A: Accelerators, Spectrometers, Detectors and Associated Equipment* 481, 765-768.
- Santisteban, J. R., Edwards, L., Fitzpatrick, M. E., Steuwer, A. & Withers, P. J., 2002b. Engineering applications of Bragg-edge neutron transmission. *Applied Physics A: Materials Science & Processing* 74, s1433-s1436.
- Santisteban, J. R., Edwards, L., Priesmeyer, H. G. & Vogel, S., 2002c. Comparison of Bragg-Edge neutron-transmission spectroscopy at ISIS and LANSCE. *Applied Physics A: Materials Science & Processing* 74, s1616-s1618.
- Santisteban, J. R., Edwards, L. & Stelmukh, V., 2006. Characterization of textured materials by TOF transmission. *Physica B: Condensed Matter* 385-386, Part 1, 636-638.
- Santisteban, J. R., Edwards, L., Steuwer, A. & Withers, P. J., 2001. Time-of-flight neutron transmission diffraction. *Journal of Applied Crystallography* 34, 289-297.
- Sato, H., Takada, O., Iwase, K., Kamiyama, T. & Kiyonagi, Y., 2010. Imaging of a spatial distribution of preferred orientation of crystallites by pulsed neutron Bragg edge transmission. *Journal of Physics: Conference Series* 251, 012070.
- Schulz, M., Böni, P., Calzada, E., Mühlbauer, M. & Schillinger, B., 2009. Energy-dependent neutron imaging with a double crystal monochromator at the ANTARES facility at FRM II. *Nuclear Instruments and Methods in Physics Research Section A: Accelerators, Spectrometers, Detectors and Associated Equipment* 605, 33-35.
- Shen, Y., Li, X., Sun, X., Wang, Y. & Zuo, L., 2012. Twinning and martensite in a 304 austenitic stainless steel. *Materials Science and Engineering: A* 552, 514-522.
- Siegmund, O. H., Vallerga, J. V., Tremsin, A. S., McPhate, J. & Feller, B., 2007. High spatial resolution neutron sensing microchannel plate detectors. *Nuclear Instruments and Methods in Physics Research Section A: Accelerators, Spectrometers, Detectors and Associated Equipment* 576, 178-182.
- Steuwer, A., Santisteban, J. R., Withers, P. J. & Edwards, L., 2004. Pattern decomposition and quantitative-phase analysis in pulsed neutron transmission. *Physica B: Condensed Matter* 350, 159-161.
- Steuwer, A., Santisteban, J. R., Withers, P. J., Edwards, L. & Fitzpatrick, M. E., 2003. In situ determination of stresses from time-of-flight neutron transmission spectra. *Journal of Applied Crystallography* 36, 1159-1168.
- Steuwer, A., Withers, P. J., Santisteban, J. R. & Edwards, L., 2005. Using pulsed neutron transmission for crystalline phase imaging and analysis. *Journal of Applied Physics* 97, 074903.
- Steuwer, A., Withers, P. J., Santisteban, J. R., Edwards, L., Bruno, G., Fitzpatrick, M. E., Daymond, M. R., Johnson, M. W. & Wang, D., 2001. Bragg Edge Determination for Accurate Lattice Parameter and Elastic Strain Measurement. *physica status solidi (a)* 185, 221-230.
- Strunz, P., Lukáš, P., Mikula, P., Wagner, V., Kouril, Z. & Vrána, M., 1997. Data Evaluation Procedure for Energy-Dispersive Neutron-Transmission-Diffraction Geometry. *Proc. of the 5th Int. Conference on Residual Stresses ICRS-5*, pp. 688-693.
- Treimer, W., Strobl, M., Kardjilov, N., Hilger, A. & Manke, I., 2006. Wavelength tunable device for neutron radiography and tomography. *Applied Physics Letters* 89, 203504.
- Tremsin, A. S., Bruce Feller, W. & Gregory Downing, R., 2005. Efficiency optimization of microchannel plate (MCP) neutron imaging detectors. I. Square channels with 10B doping. *Nuclear Instruments and Methods in Physics Research Section A: Accelerators,*

- Spectrometers, Detectors and Associated Equipment 539, 278-311.
- Tremsin, A. S., Vallerger, J. V., McPhate, J. B., Siegmund, O. H. W., Feller, W. B., Crow, L. & Cooper, R. G., 2008. On the possibility to image thermal and cold neutron with sub-15 μm spatial resolution. Nuclear Instruments and Methods in Physics Research Section A: Accelerators, Spectrometers, Detectors and Associated Equipment 592, 374-384.
- Vogel, S. (2000). Dissertation thesis, Uni Kiel, Kiel.
- Wagner, V., Kouril, Z., Lukas, P., Mikula, P., Saroun, J., Strunz, P. & Vrana, M. (1997). pp. 168-171.
- Wang, D. Q. (1996). thesis, The Open University.
- Weiss, R. J., Clark, J. R., Corliss, L. & Hastings, J., 1952. Neutron Diffraction Studies of Cold-Worked Brass. Journal of Applied Physics 23, 1379-1382.
- Winsberg, L., Meneghetti, D. & Sidhu, S. S., 1949. Total Neutron Cross Sections of Compounds with Different Crystalline Structures. Physical Review 75, 975-979.
- Zackay, V. F., Parker, E. R., Fahr, D. & Busch, R., 1967. The enhancement of ductility in high-strength steels. ASM Trans Quart 60, 252-259.